

# **Estimation Of Statistical Distributions For Modal Parameters Identified From Averaged Frequency Response Function Data**

**SCOTT W. DOEBLING AND CHARLES R. FARRAR**

*Engineering Analysis Group (ESA-EA), Los Alamos National Laboratory, Los Alamos, NM, 87545, USA*

## **Abstract**

An algorithm is presented to estimate the statistical distributions of identified modal parameters based on the random errors associated with averaged frequency response function estimates. In this study the modal parameters are assumed to be random variables and the objective is to estimate their distribution statistics (e.g. mean and variance). The algorithm first uses a classical approach to estimate the error on the averaged frequency response function using the coherence function averaged over an ensemble of measured samples. A Monte Carlo simulation approach is then used to propagate the estimated spectral function errors through the modal parameter identification process. A Bootstrap estimate of the modal parameter distribution over the full ensemble of individual measurement samples is used to verify the accuracy of the Monte Carlo algorithm. The statistics of the resulting modal parameter distribution are suitable for use as weights or filtering criteria in model correlation and damage identification schemes. Convergence criteria for determining how many Monte Carlo simulations are required are also presented and discussed. The technique is demonstrated via application to a simulated frequency response function with known parameter distributions and to experimental data from tests of an in situ bridge.

**Keywords:** Modal Parameter Estimation, Frequency Response Function, Statistics

## **Introduction**

Many applications in the fields of mechanical, aerospace, automotive, and civil engineering require the measurement of modal vibration data to allow analysts to properly model a structure or other mechanical system. The measured data sets are generally reduced to a relatively small set of modal parameters - typically modal frequencies, modal

damping ratios, and mode shapes. These parameters are then compared to analytical models to allow verification and refinement of the models.

The correlation of analytical models with measured modal parameters is important because of the uncertainty that is inherent in many engineering assumptions about physical phenomena. This uncertainty is particularly apparent in parameters describing the stiffnesses of structural joints, dynamic energy loss mechanisms (e.g. damping), and structural boundary conditions (especially when the boundaries interact with media which are difficult to analytically model, such as soil). To initially model these known uncertainties, common engineering practice is to use values that have previously been experimentally observed, simplified idealizations of the physical system, and engineering judgment. These assumptions must be used until experimental data can be obtained to judge the validity of the assumed values.

One important issue in the application of measured data to validate engineering models, which is often overlooked, is the variability inherent in the measured data and the corresponding variability in the modal parameters extracted from the data. The measured data are to some extent always subject to variability, and so there will always be some variability in the parameters extracted from different data samples. The classical approach to dealing with this variability is to assume that the modal parameters are inherently deterministic quantities and are corrupted by additive “errors” during the measurement process, as described in Bendat and Piersol (1980). In this context, the term “errors” is defined as all contributing factors (both random and systematic) that cause the measured structural response to be different than the actual structural response. If it is assumed that the errors are random, then the variability on the identified modal parameters can be expressed in terms of statistical measures such as the mean and standard deviation. Common practice is to express the random error as zero-mean and Gaussian. The mean of the measured parameter estimate is then defined to be the deterministic parameter value, with the random error expressed by statistical confidence intervals. Such intervals indicate the range of values of the parameter that one should expect to observe experimentally.

A related approach, and the one used in this paper, is to treat the modal parameters themselves as random variables, rather than treating them as deterministic quantities corrupted by random errors. This approach has a primary advantage in terms of the underlying philosophy of the structural model: This approach allows the full range of

behavior of the parameter to be represented, rather than estimating a “most likely” deterministic value. Under the deterministic approach, only a single value of each parameter is known, and thus only a single response value is calculated for the structure. However, when the parameters are treated as random variables, the behavior of the system can be predicted over the full range of values for those parameters. For example, when a modal damping value is estimated as a deterministic quantity, the model that it is used in can only predict the effects of one value of modal damping for that mode. However, estimating that same modal damping value as a random variable allows the model to predict the structure’s behavior over the appropriate range of damping values as described by its identified statistical distribution. In some applications the structural response is extremely sensitive to particular modal parameters, and thus the ability to predict the structure’s behavior over a range of values for the identified parameter is crucial. It is important to note that the standard deviations of the identified modal parameters using this type of approach are quite small, typically on the order of 0.1% - 0.2% of the estimated mean value. However, these levels of variability can be quite important in areas of study such as damage identification given the relative insensitivity of modal parameters to many types of system damage.

The question, then, is how does one compute the statistical distribution of the identified modal parameters given a set of repeated vibration measurements? Bendat and Piersol (1980) present a technique to estimate the statistical distribution of the measured frequency response function components based on the coherence function. From that point there are basically two different methods for propagating these errors through the identification process to estimate the statistics of the modal parameters: 1) Perform a sensitivity analysis of the algorithm to express the statistics of the modal parameters as linear combinations of the statistics of the FRFs, or 2) Use a sampling method to estimate the FRF statistics based on realizations of an assumed random distribution for the FRF values. Algorithms such as those presented by Longman, et al. (1988) (for the Eigensystem Realization Algorithm) and Peterson, et al. (1996) (for the Fast Eigensystem Realization Algorithm) follow the first approach by using a perturbation analysis of the entire modal identification procedure to determine the sensitivity of the modal parameters to errors in the measured data. The advantage of this approach is that the propagation of the errors is computationally efficient once the sensitivity has been computed analytically. The disadvantage to this approach is that it is mathematically complicated to compute the sensitivity of the entire procedure, and that it assumes that a

first-order approximation of the error propagation is accurate enough for a given modal parameter estimation scheme and a given data set.

The second approach, using sampling techniques to propagate errors from the FRF to the identified modal parameters, is used in this paper. Given a series of repeated FRF measurements, the Bootstrap approach (Paez and Hunter, 1998) provides an accurate estimate of the modal parameter statistics, as demonstrated on simulated data in this paper. However, this approach requires the individual FRF samples to be stored, whereas the standard protocol for the majority of commercial modal data acquisition software packages is to save only the ensemble averages of the spectral functions. (It should be noted that with the data processing and storage capabilities of modern portable computers there are typically no hardware restrictions that would prevent storage of the individual samples of the spectral functions.) To allow estimates of the modal parameters to be made for averaged FRF data, a simple procedure using Monte Carlo simulation is presented. Although the procedure is described in terms of a particular modal-parameter-identification scheme, any algorithm could be used. The accuracy of the modal parameter statistics is verified by comparison with the Bootstrap technique.

This paper is organized as follows: First, the process of spectral function and modal parameter estimation is presented, including the particular modal parameter identification algorithm used in this research. Next, the procedure for estimating the statistics on the measured spectral functions is outlined, including a discussion of the sources of measurement error. Next, the procedure for propagating the statistics to the identified modal parameters from the individual samples of the repeated FRF measurements using the Bootstrap technique is presented, followed by the corresponding technique to estimate the modal parameter statistics from averaged FRF data using the Monte Carlo approach. Finally, the Monte Carlo and Bootstrap techniques are verified by application to simulated FRF data with known modal parameter statistics and validated by application to measured modal data from the Alamosa Canyon bridge tests.

## **Identification Of Modal Parameters From Spectral Estimates**

As described in the introduction, it is often desirable to measure vibration data from a structure and then reduce the results of these measurements to a relatively small set of modal frequencies, modal damping ratios, and mode

shapes. As described by McConnell (1995), the first step in this procedure is to obtain measured excitation time histories  $x(t)$  (typically in units of force) and the measured response time histories  $y(t)$  (typically in units of acceleration) using appropriate sampling, windowing, and filtering procedures. The estimation of frequency-domain measurement functions follows with the computation of the auto-power spectral density function estimates  $\hat{G}_{xx}(\omega)$  and  $\hat{G}_{yy}(\omega)$  and the cross-power spectral density function estimates  $\hat{G}_{xy}(\omega)$ . The next step in this procedure is the estimation of the FRF (the normalized frequency-domain input-output relationship) and coherence function (a normalized measure of the linearity between the excitation signal and the response signal that takes on a value between 0 and 1) for each  $x$ - $y$  pair. There are many different ways of estimating the FRF based on the assumptions about the primary sources of random error in the measurements. The most common FRF estimate, based on the assumption that the random error on the excitation signal measurement is small, is the so-called  $H_1$  FRF estimate

$$\hat{H}_{xy}(\omega) = \frac{\hat{G}_{xy}(\omega)}{\hat{G}_{xx}(\omega)} \quad (1)$$

The corresponding coherence function estimates can be computed as

$$\hat{\gamma}_{xy}^2(\omega) = \frac{|\hat{G}_{xy}(\omega)|^2}{\hat{G}_{xx}(\omega)\hat{G}_{yy}(\omega)} \quad (2)$$

Any deviation from the linear input-output relationship of the structure such as those that may arise from nonlinearities, unmeasured excitations, or signal processing procedures will degrade the value of the coherence function away from 1. This occurrence is commonly referred to as “loss of coherence.” As explained in the next section, the spectral density function estimates  $\hat{G}_{xx}(\omega)$ ,  $\hat{G}_{yy}(\omega)$ , and  $\hat{G}_{xy}(\omega)$ , are averaged over several instances of excitation to minimize random errors. Thus the values used for the computations in equation (1) and equation (2) are typically not the actual values  $G_{xx}(\omega)$ ,  $G_{yy}(\omega)$ , and  $G_{xy}(\omega)$ , but rather are “estimates” obtained by observing the signals over several instances of excitation and averaging the results.

The identification of modal parameters from the estimated FRF is accomplished by any number of methods that fit an analytical modal model to the measured FRF data, as described by Maia and Silva (1997). Some methods fit the FRF directly, while others fit the inverse discrete Fourier transform, known as the discrete unit impulse response function. The method used to identify modal parameters in this paper is the Rational Polynomial curve fit, as presented originally by Richardson and Formenti (1982) although, as stated previously, any modal parameter identification algorithm could be used. The Rational Polynomial curve fit is based on the expression of the FRF between a given input- output pair as a ratio of two polynomials. This expression can be written as

$$H_{xy}(\omega) = \frac{\sum_{k=0}^m a_k (j\omega)^k}{\sum_{k=0}^n b_k (j\omega)^k} \quad (3)$$

$$n = 2p$$

$$m = 2p - 1 + r$$

where  $p$  is the number of modes and  $r$  is the number of residual terms. The residual terms account for the influence of modes which are located outside the curve-fit bandwidth. The rational polynomial form of Eq. (3) can be converted to pole-residue form and from there the modal parameters can be extracted. There is one denominator polynomial for the entire set of data because each FRF has the same pole locations that are functions of the modal frequencies and modal damping ratios. However, each DOF has a different numerator polynomial because each FRF has different residues that are functions of the mode shape amplitudes.

### **Estimation Of Statistical Distributions For Measured Spectral Functions**

As mentioned in the introduction, measured data contain errors caused by many sources that result in measured spectral function estimates that are not equal to the actual spectral functions of the structure. The errors that are present in the measured modal data can be divided into two basic categories, as described in Bendat and Piersol (1980): bias (systematic) errors and random errors. Bias errors cause the mean of the function estimate not to converge to the actual value of the function as more averages are taken. Random errors, however, are those error

components that will tend to cancel out as more averages are taken. Bias errors arise primarily from the following sources:

1. Electrical noise in the excitation measurement that does not produce a physical response
2. Bias in the spectral density estimates resulting from inadequate spectral (sampling) resolution
3. System nonlinearities
4. Unmeasured excitations that contribute to the response and are correlated with the measured excitation
5. Errors related to signal processing such as aliasing and leakage

Random errors arise primarily from 3 sources:

1. Electrical noise in the sensors and signal processing, and digital noise in the sampling process
2. Unmeasured excitations that contribute to the response and are uncorrelated with the measured excitation
3. System nonlinearities

Many standard modal testing practices are used to minimize the effects of the bias errors. For example, filtering and windowing can minimize the effects of aliasing and leakage, respectively. Presuming that the data acquisition parameters and signal processing procedures are chosen so that the bias errors are minimized, and assuming that the FRF estimate in equation (1) is used and that structural linearity and reciprocity are verified for the measured bandwidth, then the primary source of errors will be random errors arising from unmeasured excitations. Using the assumption that the primary errors are random and uncorrelated with the excitation and structural responses, and that the excitation input is from a single source, the confidence intervals  $\sigma_{\mu}$  on the estimate of the mean FRF magnitude and phase random are (according to Bendat and Piersol, 1980):

$$\begin{aligned}\sigma_{\mu} \left( \left| \hat{H}_{xy}(\omega) \right| \right) &= \frac{\sqrt{1 - \gamma_{xy}^2(\omega)}}{\left| \gamma_{xy}(\omega) \right| \sqrt{2n_d}} \left| \hat{H}_{xy}(\omega) \right| \\ \sigma_{\mu} \left( \angle \hat{H}_{xy}(\omega) \right) &= \sin^{-1} \left( \frac{\sqrt{1 - \gamma_{xy}^2(\omega)}}{\left| \gamma_{xy}(\omega) \right| \sqrt{2n_d}} \right)\end{aligned}\quad (4)$$

where  $n_d$  is the number of measured FRF samples. Typically a particular statistical distribution is assumed, so that a percentage confidence level can be associated with the confidence intervals  $\sigma_{\mu}$ . In practice, because the true coherence functions  $\gamma_{xy}^2(\omega)$  are unknown, the estimates  $\hat{\gamma}_{xy}^2(\omega)$  defined in equation (2) are used instead. This substitution produces accurate confidence interval estimates when the confidence interval estimate is approximately 20% or less of the mean estimate for a particular parameter. As a practical matter, the argument of the arcsin function in equation (4) must be constrained to be less than 1.

It should be noted that the formulae in equation (4) are estimates of the confidence intervals on the mean of the magnitude and phase, NOT estimates of the standard deviation of the magnitude and phase, assuming that the magnitude and phase themselves are Gaussian-distributed random variables. As derived in Bevington and Robinson (1992), the relationship between the estimate of the population standard deviation,  $\sigma$ , and the confidence interval on the mean estimate,  $\sigma_{\mu}$ , is given as

$$\sigma_{\mu} = \frac{\sigma}{\sqrt{n_d}} \quad (5)$$

Thus, the estimates of the standard deviations of the FRF magnitude and phase are

$$\begin{aligned}\sigma \left( \left| \hat{H}_{xy}(\omega) \right| \right) &= \frac{\sqrt{1 - \gamma_{xy}^2(\omega)}}{\left| \gamma_{xy}(\omega) \right| \sqrt{2}} \left| \hat{H}_{xy}(\omega) \right| \\ \sigma \left( \angle \hat{H}_{xy}(\omega) \right) &= \sin^{-1} \left( \frac{\sqrt{1 - \gamma_{xy}^2(\omega)}}{\left| \gamma_{xy}(\omega) \right| \sqrt{2}} \right)\end{aligned}\quad (6)$$



It is noted by comparing equations (6) and (4) that they differ by the factor  $\sqrt{n_d}$  as described in Equation (5). For the phase, this factor is applied to the operand of the arcsin function because the relationship of Equation (5) is applied to the relative error terms, from which the standard deviation estimates of equations (6) are derived.

## **Propagation of estimated errors in modal parameter identification**

In the previous section, the statistics on the spectral function errors were estimated. The next step is to propagate those errors through the modal parameter identification procedure using a sampling technique to estimate the statistical distributions of those parameters. As described in the introduction, there are two basic procedures that can be used to accomplish the propagation: Bootstrap simulation using the individual measured FRF samples, or Monte Carlo simulation using the ensemble average FRF estimates. Each of these procedures is outlined in this section, along with discussions of their advantages and disadvantages. The Bootstrap method is more accurate because it does not assume the form of the parameter distribution, but the Monte Carlo method can be applied to averaged modal data, which is of interest in many practical applications.

The more accurate sampling approach for the propagation of FRF statistics to modal parameter statistics is the Bootstrap approach as presented in Paez and Hunter (1998). The Bootstrap analysis procedure randomly selects individual FRF measurements to form the ensemble average. Because the FRFs for a particular DOF are selected at random and “with replacement,” a single FRF sample may be used more than once in the ensemble average while others may not be included. This process results in ensemble averages that are based on random weighting of the sample FRFs. The individual FRF samples are required (rather than the ensemble average FRF spectra). This Bootstrap approach is advantageous because it does not require an assumption of the form of the FRF statistical distribution because of the random FRF weighting. Once the randomly weighted ensemble averages are formed for each DOF, the modal parameter identification procedure is applied. This procedure is repeated numerous times to form a histogram of the identified modal parameters. Statistics for the distribution of the modal parameters can be estimated from this histogram.

The steps used to implement the Bootstrap procedure are shown in Figure 1 and described here:

1. Measure and store  $n_d$  FRF samples (acquired at each DOF simultaneously).
2. Randomly select  $n_d$  of the  $n_d$  FRFs, with replacement, and form an ensemble average (using the same  $n_d$  FRFs at each DOF).
3. Apply the modal parameter identification procedure to this ensemble average to estimate a set of modal parameters (resonant frequencies, modal damping, mode shape amplitudes and phases).
4. Repeat steps 1-3 and form a histogram for each modal parameter.
5. Calculate the statistics of the distribution represented by this histogram to check for convergence.

Note that no assumption on the distribution of the identified parameters, no assumption about the form of the input or response, and no assumption about the number of inputs or responses are made in this analysis. The Bootstrap method does require each individual FRF sample to be stored, which is sometimes difficult to accomplish with commercial modal data-acquisition software.

An alternative to the Bootstrap approach is required for the case when only the averaged FRFs are available (which is the majority of cases). In this situation, the Monte Carlo simulation technique derived here can be used as an alternative. As described in Press, et al. (1992), Monte Carlo simulation is a procedure whereby noisy data sets are repeatedly “simulated” using the assumed statistical distribution of error on the data. The identification procedure is then applied to each of the simulated data sets, producing a set of identified model parameters. After a sufficient number of simulations, the distribution of the resulting set of identified model parameters is assumed to be representative of the distribution of the true model parameters plus the effects of the measurement errors.

The basic procedure for the Monte Carlo simulation used in this analysis is shown in Figure 2 and described here. In the previous section, the statistical distributions on the measured FRFs were defined. These assumed distributions are the basis for the generation of data sets for the Monte Carlo simulation. First, the mean and standard deviation on the FRF magnitude and phase, computed using equation (4), are used to generate a “noisy” FRF  $\tilde{H}_{xy}(\omega)$  as

$$\tilde{H}_{xy}(\omega) = \left| \tilde{H}_{xy}(\omega) \right| e^{j\angle \tilde{H}_{xy}(\omega)} \quad (7)$$

where the magnitude and phase components are drawn from a multivariate Gaussian random population  $R$  with the following statistics:

$$\mu_R = \begin{bmatrix} \mu \left( \left| \hat{H}_{xy}(\omega) \right| \right) \\ \mu \left( \angle \hat{H}_{xy}(\omega) \right) \end{bmatrix} \quad \Sigma_R = \text{diag} \left( \sigma^2 \left( \left| \hat{H}_{xy}(\omega) \right| \right), \sigma^2 \left( \angle \hat{H}_{xy}(\omega) \right) \right) \quad (8)$$

The simulated FRF  $\tilde{H}_{xy}(\omega)$  is then used for the identification of a set of modal parameters using any modal parameter identification scheme, although the Rational Polynomial curve fit is used for this research. (In the case of multiple DOF, all of the individual FRFs are included in equation (8).) The resulting modal frequencies, modal damping ratios, and mode shapes are stored for each simulation and histograms are accumulated. This procedure is repeated until the statistics on the modal parameters converge.

There is one primary drawback to the Monte Carlo simulation approach: The method requires an assumption of the form of the distribution (in this case Gaussian) of the variability of the FRF samples. However, it will operate on averaged FRF data whereas the Bootstrap will not. Finally, it should be noted that both the Monte Carlo and the Bootstrap procedures will not account for bias errors introduced by signal processing (for example, those introduced by windowing functions) or for bias errors introduced during the parameter estimation procedure.

Defining the criteria for determining when the results of the Monte Carlo and Bootstrap simulations have converged is important. These criteria are used to set the limits at which the simulation runs should cease. The criteria are established by monitoring the convergence of the first four statistical moments of the modal parameter distributions. The first moment is the mean and the second moment is the standard deviation, computed as described in any elementary statistics textbook. The third moment (distribution skewness) is estimated as

$$\text{Skew}(x) = \frac{1}{N} \sum_{j=1}^N \left[ \frac{x_j - \bar{x}}{\sigma} \right]^3 \quad (9)$$

and the fourth moment (distribution kurtosis or flatness) is estimated as

$$\text{Kurt}(x) = \left\{ \frac{1}{N} \sum_{j=1}^N \left[ \frac{x_j - \bar{x}}{\sigma} \right]^4 \right\} - 3 \quad (10)$$

(In these equations,  $x$  is the vector of modal parameters from the Monte Carlo or Bootstrap simulations,  $\bar{x}$  and  $\sigma$  are the mean and standard deviation of this vector, and  $N$  is the number of Monte Carlo or Bootstrap simulations.) For a perfect Gaussian distribution, the skewness and kurtosis will both be zero. Press, et al. (1992) suggest that a distribution with a skewness less than  $\sqrt{15/N}$  and kurtosis less than  $\sqrt{96/N}$  can be considered to be a Gaussian distribution. The convergence of these four statistical moments are the quantitative measures used in this paper to determine that a sufficient number of Monte Carlo and Bootstrap simulations have been performed. If the skewness and kurtosis converge to within the specified tolerances for a particular parameter, then that parameter's distribution is considered to be Gaussian.

### Application To Simulated Frequency Response Function Data

To demonstrate the proposed method, it is first applied to a sequence of FRF's generated with modal frequencies and damping drawn randomly from a known Gaussian population. The objective of the demonstration is to show that the correct random distributions for these parameters are obtained from the identification procedure. The formula used to generate the FRFs is:

$$H_{xy}(\omega) = \left( \frac{A_n}{j\omega - p} + \frac{A_n^*}{j\omega - p^*} \right) \omega^2 \quad (11)$$

$$p = \omega_n \left( -\zeta_n + j\sqrt{1 - \zeta_n^2} \right)$$

where  $\omega_n$ ,  $\zeta_n$ , and  $A_n$  are the modal frequency, damping ratio, and residue for the  $n^{\text{th}}$  mode, respectively,  $j = \sqrt{-1}$  and  $( )^*$  represents complex conjugate. The modal parameter distribution statistics are given in Table 1. For the example,  $n_d = 30$  FRFs are generated for 1 mode, and are shown in Figure 3. For the Bootstrap analysis, a random sampling of the  $n_d = 30$  FRFs are selected in each simulation. The selected FRFs are averaged and a set

of modal parameters is identified from the averaged FRF. This procedure is repeated  $n_{boot}$  times. For the Monte Carlo analysis, a mean and standard deviation are defined from the  $n_d$  generated FRFs (shown in Figure 4), then this new distribution is sampled to obtain the  $n_{mc}$  number of FRFs for the Monte Carlo run. A set of modal parameters is then extracted from each of the  $n_{mc}$  Monte Carlo FRFs.

The results of the two methods are shown in Table 1 alongside the known statistics for the parameters. Figure 5 shows convergence plots for the mean and standard deviation of the modal frequency and modal damping parameters. The convergence of the distribution's kurtosis is shown in Figure 6. The convergence of the first modal frequency mean with +/- 2 STD bounds is shown in Figure 7. All of these plots indicate that a) both the MC and Bootstrap simulations have converged, and b) both the MC and Bootstrap approaches yield the correct statistics for the identified modal parameters to within a reasonable tolerance. These results verify that both the Bootstrap and Monte Carlo algorithms will identify the correct statistical distributions when the parameters are generated from known distributions.

## **Experimental Implementation And Validation**

In this section the verified Monte Carlo and Bootstrap approaches will be applied to experimentally measured data from the Alamosa Canyon Bridge. The results will demonstrate that the Monte Carlo technique produces statistics from the averaged FRF data that are comparable to those obtained from the individual FRF samples using the Bootstrap technique. Thus, the validity of the Monte Carlo approach will be demonstrated on experimental data.

The Alamosa Canyon Bridge has seven independent spans with a common pier between successive spans. An elevation view of the bridge is shown in Figure 8 along with a diagram of the bridge cross section. Each span consists of a concrete deck supported by six W30x116 steel girders. The roadway in each span is approximately 7.3 m (24 ft) wide and 15.2 (50 ft) long. A concrete curb and guardrail are integrally attached to the deck. Four sets of cross braces are equally spaced along the length of the span between adjacent girders. The cross braces are channel sections (C12x25). The bridge is aligned in a north-south direction.

The data acquisition system and measurement hardware described in Farrar, et al. (1997) were set up to measure acceleration- and force-time histories. FRFs and coherence functions were then calculated from the measured quantities. Sampling parameters were specified that calculated the FRFs from a 16-s time window discretized with 2048 samples. The FRFs were calculated for a frequency range of 0 to 50 Hz. These sampling parameters produced a frequency resolution of 0.0625 Hz. A Force window was applied to the signal from the hammer's force transducer and exponential windows were applied to the signals from the accelerometer. AC coupling was specified to minimize DC offsets.

A total of 31 acceleration measurements were made on the concrete deck and on the girders below the bridge as shown in Figure 9. Five accelerometers were spaced along the length of each girder. Because of the limited number of data channels, measurements were not made on the girders at the abutment or at the pier. Excitation was applied in the vertical direction on the top surface of the deck with an instrumented hammer. The force-input and acceleration-response time histories obtained from each impact were subsequently transformed into the frequency domain so that the FRFs and coherence functions could be estimated. Thirty averages were used for these estimates. With the sampling parameters listed above and the overload reject specified, data acquisition for a specific test usually occurred over a time period of approximately 30 - 45 minutes.

Observation of the modal parameters of the bridge over time indicated that there was variability inherent in the response of the structure. Figure 10 shows the variability of the first modal frequency with time and temperature differential. The obvious variation of the bridge modal parameters with time and temperature demonstrates that for this structure it is legitimate to treat the modal parameters as random variables. A more in-depth treatment of the temperature-dependent variability is presented by Cornwell, et al. (1999). Because the 30 FRF samples from each ACBT test were saved individually (no averaging), the Bootstrap method can be applied directly. For each Bootstrap simulation, a sample of 30 FRFs are drawn randomly with replacement from the set of 30 measured FRFs shown in Figure 11. The results of the Bootstrap simulation are shown in Table 2. The Bootstrap results are considered here to accurately represent the distribution of the identified modal parameters over the ensemble of 30 samples acquired.

Given that during most modal tests only the averaged data are saved, it is interesting to see how accurately the distributions of the modal parameters can be obtained from the averaged FRF data. To obtain the modal parameter

statistics from the averaged data, it is necessary to implement the Monte Carlo approach derived above. First, the distributions on the FRF components are computed using Equations (6). The mean and standard deviation bounds are shown for a typical FRF channel in Figure 12, along with the corresponding coherence function. Applying the Monte Carlo method results in the modal parameter statistics shown in Table 2. The convergence of Mode 1 frequency and damping ratio for both the Monte Carlo and Bootstrap approaches is shown in Figure 13, and the convergence of the kurtosis statistics is shown in Figure 14. The convergence of the mean of modal frequency 1 +/- 2 STD is shown in Figure 15. The other two identified modes show similar convergence.

Inspection of the convergence plots indicates that the number of simulation runs used was sufficient for both the Monte Carlo and Bootstrap techniques. The convergence of the kurtosis, in particular, indicates that the distributions of the identified modal parameters can be considered to be Gaussian. Overall, the Monte Carlo statistics show good agreement with the Bootstrap statistics. Thus, the Monte Carlo approach presented here provides adequate estimates of the statistics of the identified modal parameters from averaged frequency response function data.

## **Conclusions and Issues**

This paper has presented a method for computing statistical distributions for modal parameters identified from averaged frequency response function data. The method compares favorably to the previously derived Bootstrap technique. This algorithm can be used to obtain statistical distributions from any averaged FRF data provided only that the averaged coherence functions are also saved, although it is preferable to save the individual FRF samples and perform a Bootstrap analysis. This approach treats the modal parameters as inherently random variables rather than deterministic quantities corrupted by random noise, which is fundamentally different than previous approaches to quantifying the statistics of modal parameter estimates. This approach can be implemented with any modal parameter curve-fitting method. An application of this technique that is under further investigation is the separation of random parameter fluctuations caused by noise from those caused by changes in the environment of the structure. Finally, it should be noted that the error captured in the coherence function is only a measure of that error attributable to random sources. Also, influences other than random error (such as nonlinearity) can cause losses in coherence and thus overestimation of the variability of the identified parameters. Overall, the approach presented here appears to be an effective way to determine statistics on identified modal parameters.

## Acknowledgments

Los Alamos National Laboratory Directed Research and Development Project #95002 provided support for this work. This work was performed under the auspices of the United States Department of Energy.

## References

Bendat, J.S. and Piersol, A.G., 1980, *Engineering Applications of Correlation and Spectral Analysis*, Wiley, New York, p. 274.

Bevington, P.R. and Robinson, D.K., 1992, *Data Reduction and Error Analysis for the Physical Sciences*, 2<sup>nd</sup> ed., WCB/McGraw-Hill, Boston, MA.

Cornwell, P.J., Farrar, C.R., Doebling, S.W., and Sohn, H., 1999, "Environmental variability of modal properties," *Experimental Techniques*, v. 23(#6), Nov/Dec, pp. 45-48.

Farrar, C. R., Doebling, S. W., Cornwell, P. J., and Straser, E. G., 1997, "Variability of modal parameters measured on the alamosa canyon bridge," in *Proceedings 15th International Modal Analysis Conference*, Orlando, FL, pp. 257-263.

Longman, R.W., Bergmann, M., and Juang, J.-N., 1988, "Variance and bias confidence criteria for era modal parameter identification," in *Proceedings of AIAA Astrodynamics Conference*, AIAA Paper No. 88-4312-CP, pp. 729-739.

Maia, N. M. M. and Silva, J. M. M., 1997, *Theoretical and Experimental Modal Analysis*. Wiley, New York.

McConnell, K.G., 1995, *Vibration Testing: Theory and Practice*, Wiley, New York, Ch. 2.

Paez T.L and Hunter N.F., 1998, "Statistical series: part-5: fundamental-concepts of the bootstrap for statistical-analysis of mechanical systems," *Experimental Techniques*, 22(3), 35-38.



Peterson, L.D., Bullock, S.J., and Doebling, S.W., 1996, "The statistical sensitivity of experimental modal frequencies and damping ratios to measurement noise," *Modal Analysis: The International Journal of Analytical and Experimental Modal Analysis*, 11(1), 63-75.

Press, W.H., Teukolsky, S.A., Vetterling, W.T., and Flannery, B.P., 1992, *Numerical Recipes in FORTRAN*, 2nd ed., Cambridge University Press, Cambridge, UK, pp. 605-607, 684-686.

Richardson, M.H. and Formenti, D.L., 1982, "Parameter estimation from frequency response measurements using rational fraction polynomials," in *Proceedings of 1st International Modal Analysis Conference*, Society for Experimental Mechanics, Bethel, CT, pp. 167-181.

## Tables & Figures

**Table 1: Statistics of Identified Parameters for Random Simulated FRFs**

	Mean (1 <sup>st</sup> Moment)	Standard Deviation (2 <sup>nd</sup> Moment)	Skewness (3 <sup>rd</sup> Moment) < $\sqrt{15/n_d}$	Kurtosis (4 <sup>th</sup> Moment) < $\sqrt{96/n_d}$
Population Modal Frequency (Hz)	5.00	0.0100	Yes	Yes
Identified Modal Frequency, Bootstrap (Hz)	5.00	0.011	No	No
Modal Frequency Error, Bootstrap (%)	0.0480 %	10.0 %		
Identified Modal Frequency, Monte Carlo (Hz)	5.00	0.0109	Yes	Yes
Modal Frequency Error, Monte Carlo (%)	0.0500 %	9.40 %		
Population Modal Damping	0.0100	0.00100	Yes	Yes
Identified Modal Damping, Bootstrap	0.00992	0.00118	No	Yes
Modal Damping Error, Bootstrap(%)	0.799 %	17.5 %		
Identified Modal Damping, Monte Carlo	0.00992	0.00121	No	No
Modal Damping Error, Monte Carlo (%)	0.840 %	21.0 %		

**Table 2: Statistics of Identified Parameters for Alamosa Canyon Bridge FRFs**

	Mean (1 <sup>st</sup> Moment)	Standard Deviation (2 <sup>nd</sup> Moment)	Skewness (3 <sup>rd</sup> Moment) < $\sqrt{15/n_d}$	Kurtosis (4 <sup>th</sup> Moment) < $\sqrt{96/n_d}$
Mode 1 Frequency, Bootstrap (Hz)	7.303	0.0096	Y	Y
Mode 1 Frequency, Monte Carlo (Hz)	7.301	0.0098	Y	Y
Mode 1 Frequency Difference <sup>†</sup> (%)	-0.02%	2.08%		
Mode 1 Damping, Bootstrap (Hz)	0.0184	0.0011	Y	Y
Mode 1 Damping, Monte Carlo (Hz)	0.0174	0.0014	N	Y
Mode 1 Damping Difference (%)	-5.43%	27.27%		
Mode 2 Frequency, Bootstrap (Hz)	8.122	0.0161	N	Y
Mode 2 Frequency, Monte Carlo (Hz)	8.111	0.0128	Y	Y
Mode 2 Frequency Difference (%)	-0.13%	-20.50%		
Mode 2 Damping, Bootstrap (Hz)	0.0174	0.0019	N	Y
Mode 2 Damping, Monte Carlo (Hz)	0.0166	0.0019	Y	Y
Mode 2 Damping Difference (%)	-4.60%	0.00%		

---

<sup>†</sup> Difference = (Bootstrap – Monte Carlo) / Bootstrap x 100%

Mode 3 Frequency, Bootstrap (Hz)	11.600	0.0117	N	Y
Mode 3 Frequency, Monte Carlo (Hz)	11.598	0.0115	Y	Y
Mode 3 Frequency Difference (%)	-0.02%	-1.71%		
Mode 3 Damping, Bootstrap (Hz)	0.0102	0.0013	Y	Y
Mode 3 Damping, Monte Carlo (Hz)	0.0097	0.0009	N	Y
Mode 3 Damping Difference (%)	-4.90%	-30.77%		

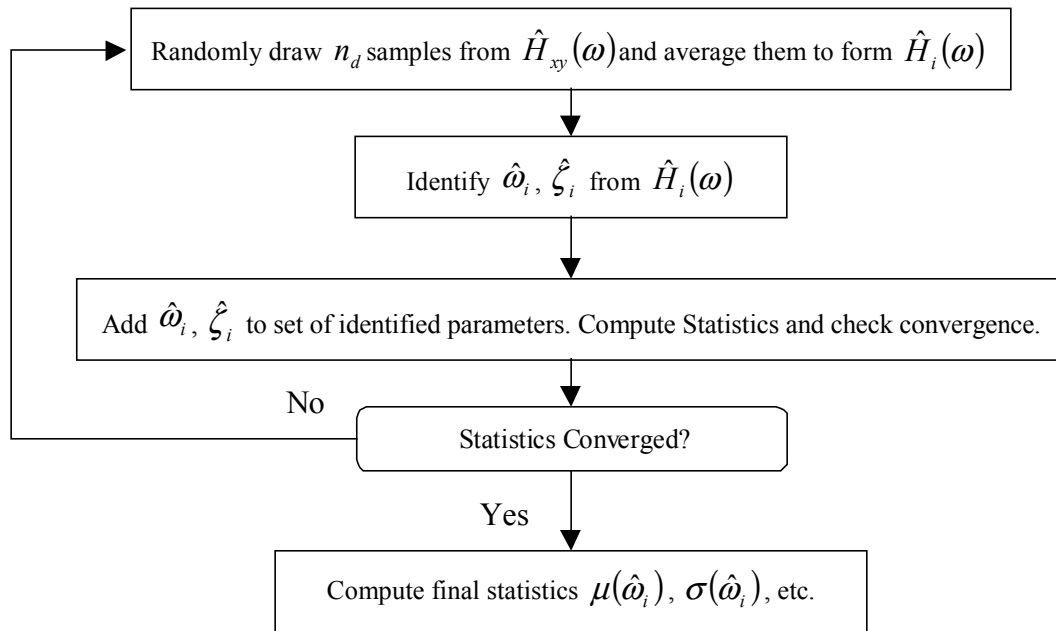


**Figure 1: Flowchart of Bootstrap Procedure for Estimating Statistical Distributions**

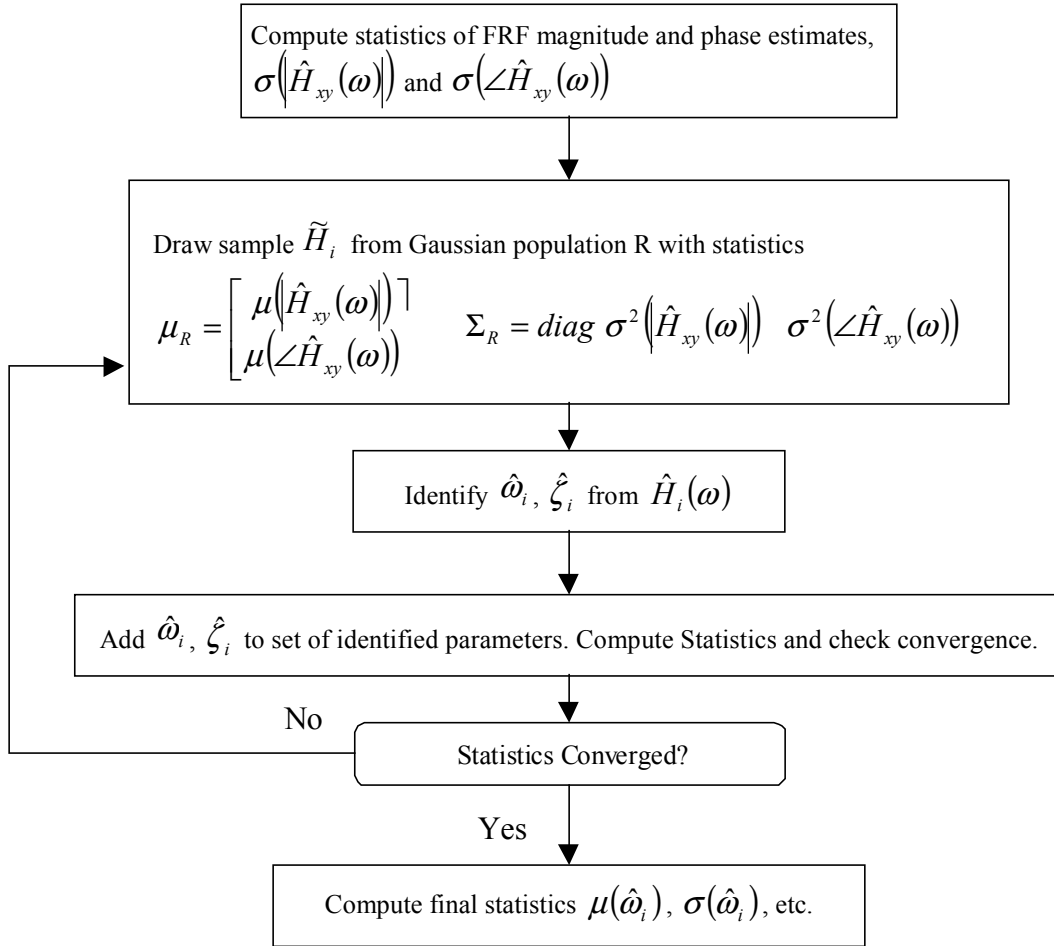


**Figure 2: Flowchart of Monte Carlo Procedure for Propagating Statistical Distributions**

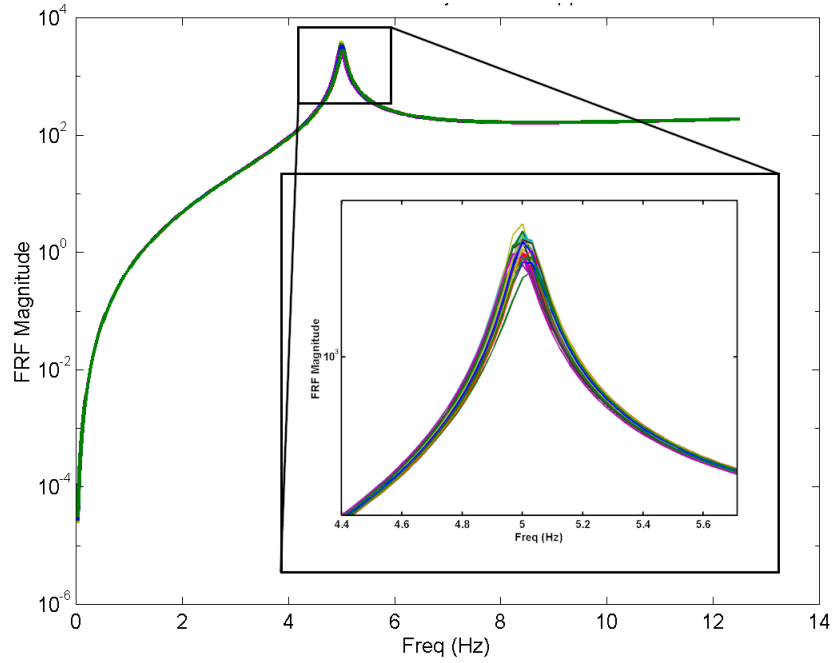


**Figure 3: Simulated Frequency Response Functions for Bootstrap Analysis**

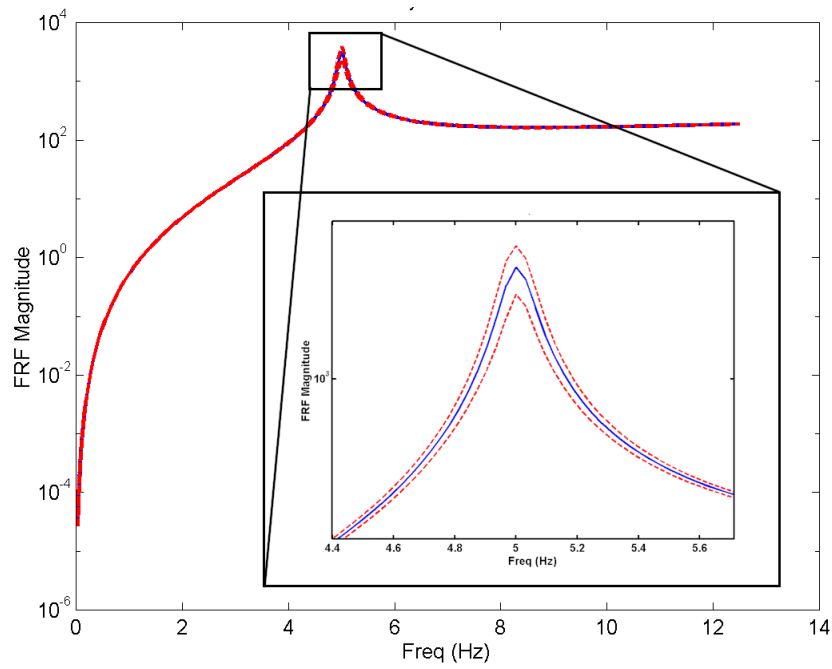


**Figure 4: Simulated Frequency Response Function Bounds (2 STD) for Monte Carlo Analysis**

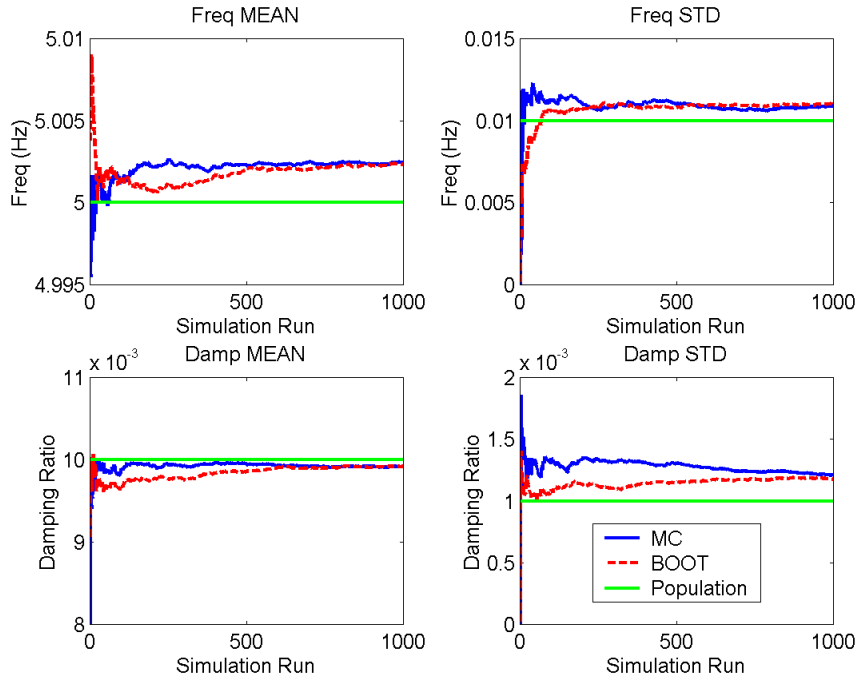


**Figure 5: Convergence of Modal Parameter Statistics for Simulated Frequency Response Data**

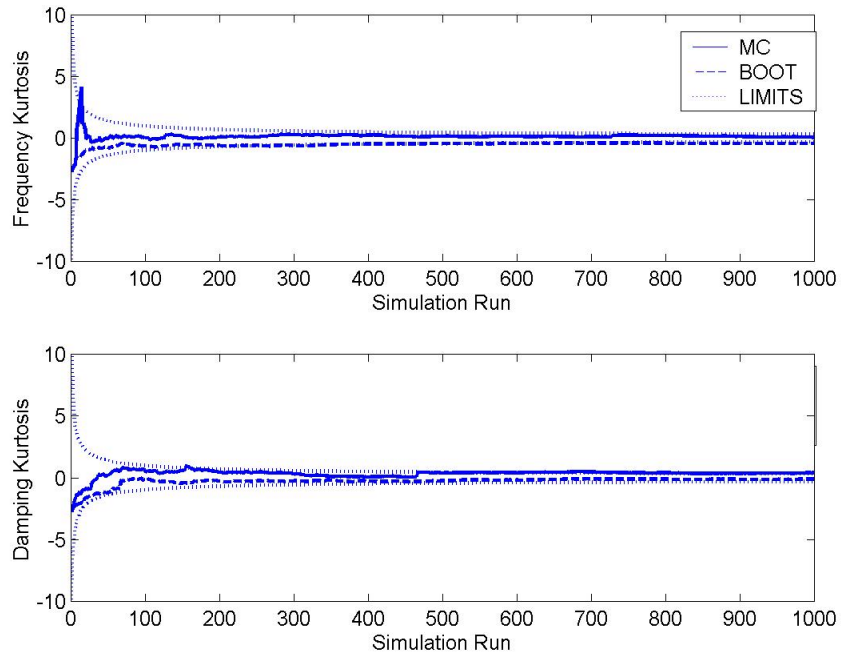


**Figure 6: Convergence of Modal Parameter Kurtosis for Simulated Frequency Response Data**



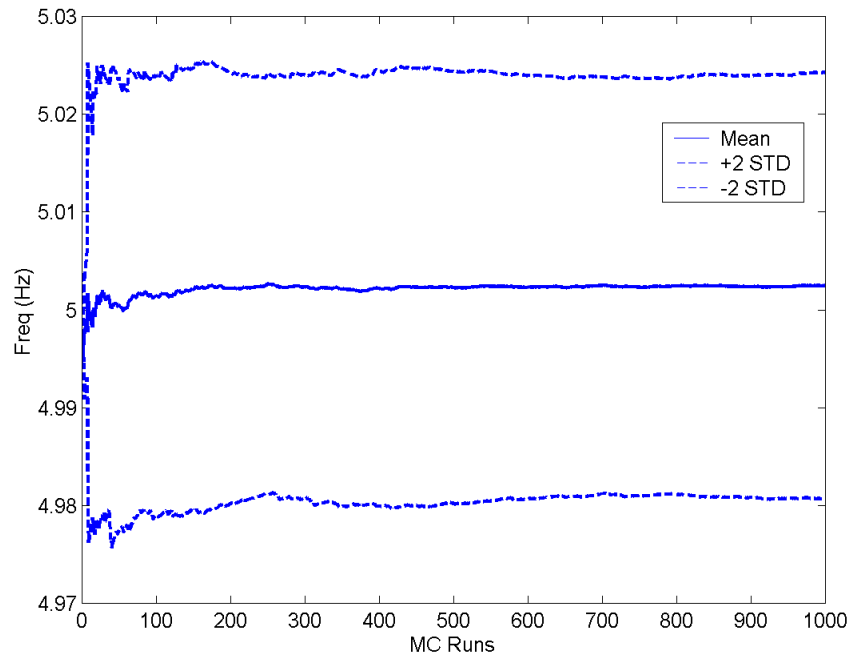


**Figure 7: Convergence of First Modal Frequency for Simulated Frequency Response Data**

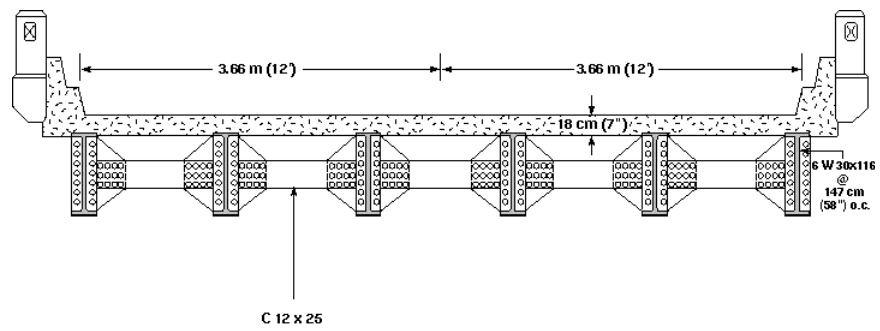


**Figure 8: Elevation View and Cross Section of the Alamosa Canyon Bridge**

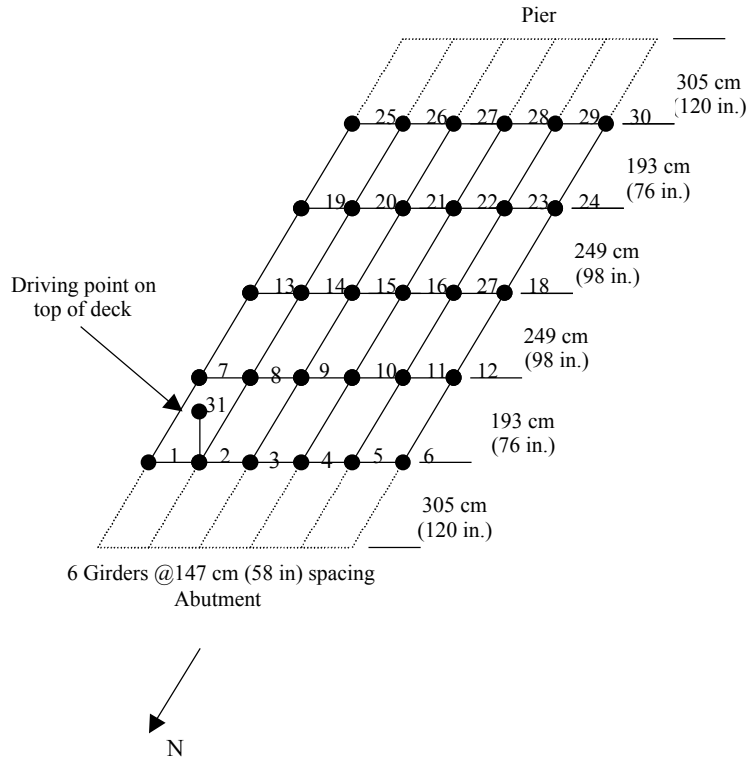


**Figure 9: Sensor Layout for Alamosa Canyon Bridge Tests**

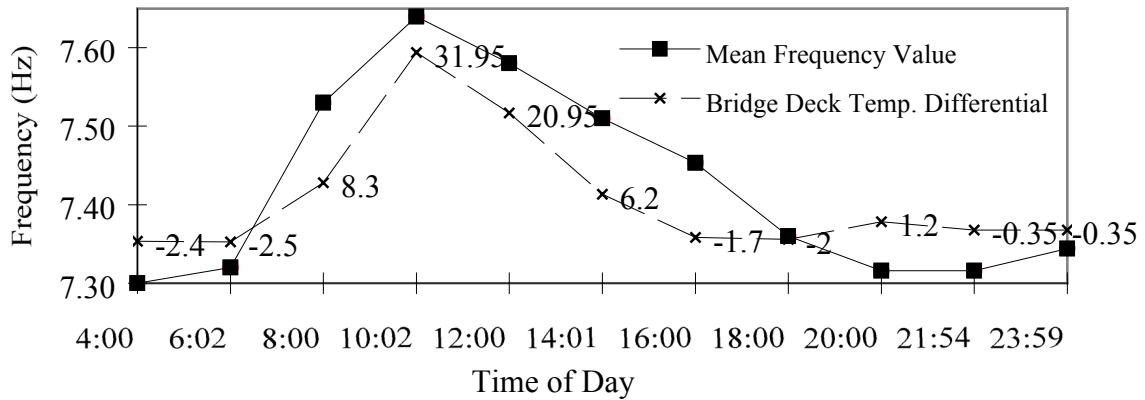


**Figure 10: Variability of First Modal Frequency with Time and Temperature Differential**

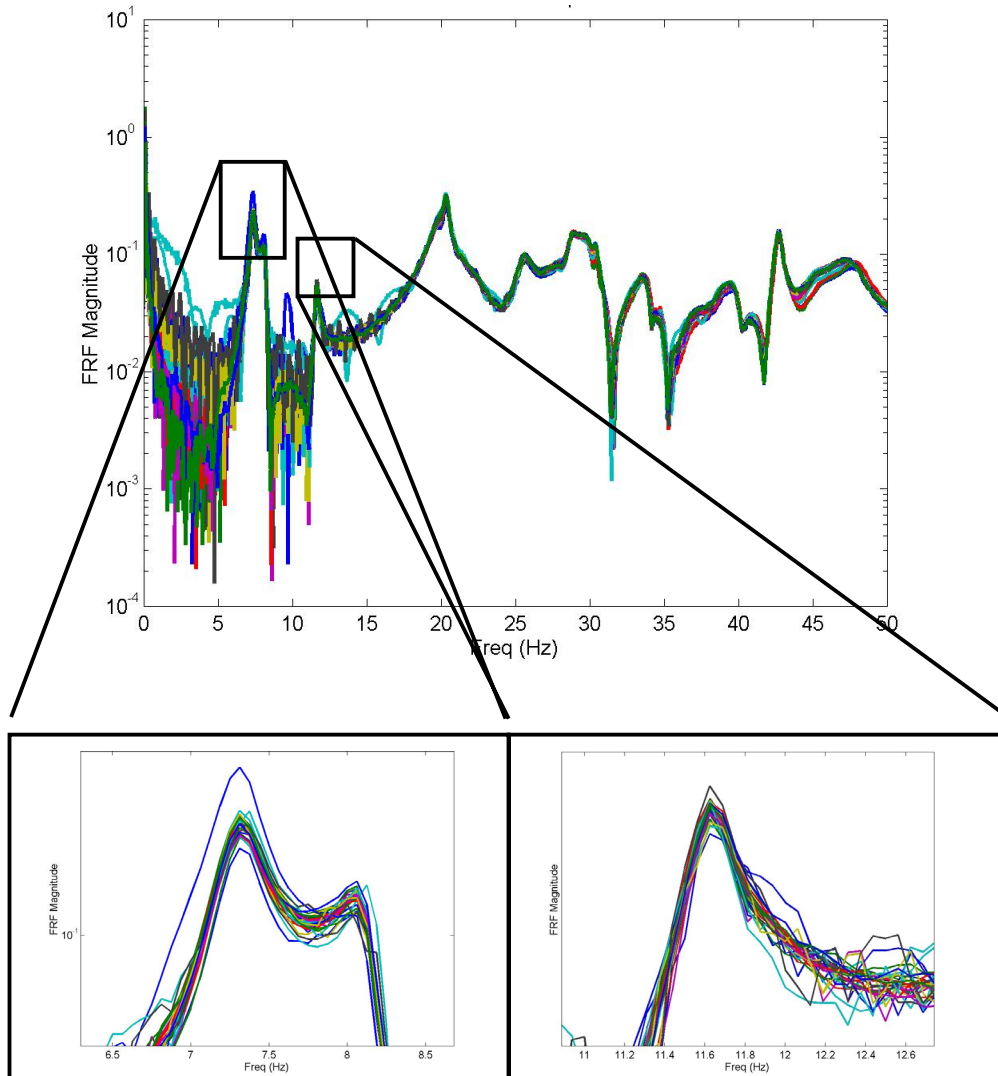


**Figure 11: Individual FRF Samples from Alamosa Canyon Bridge Test**

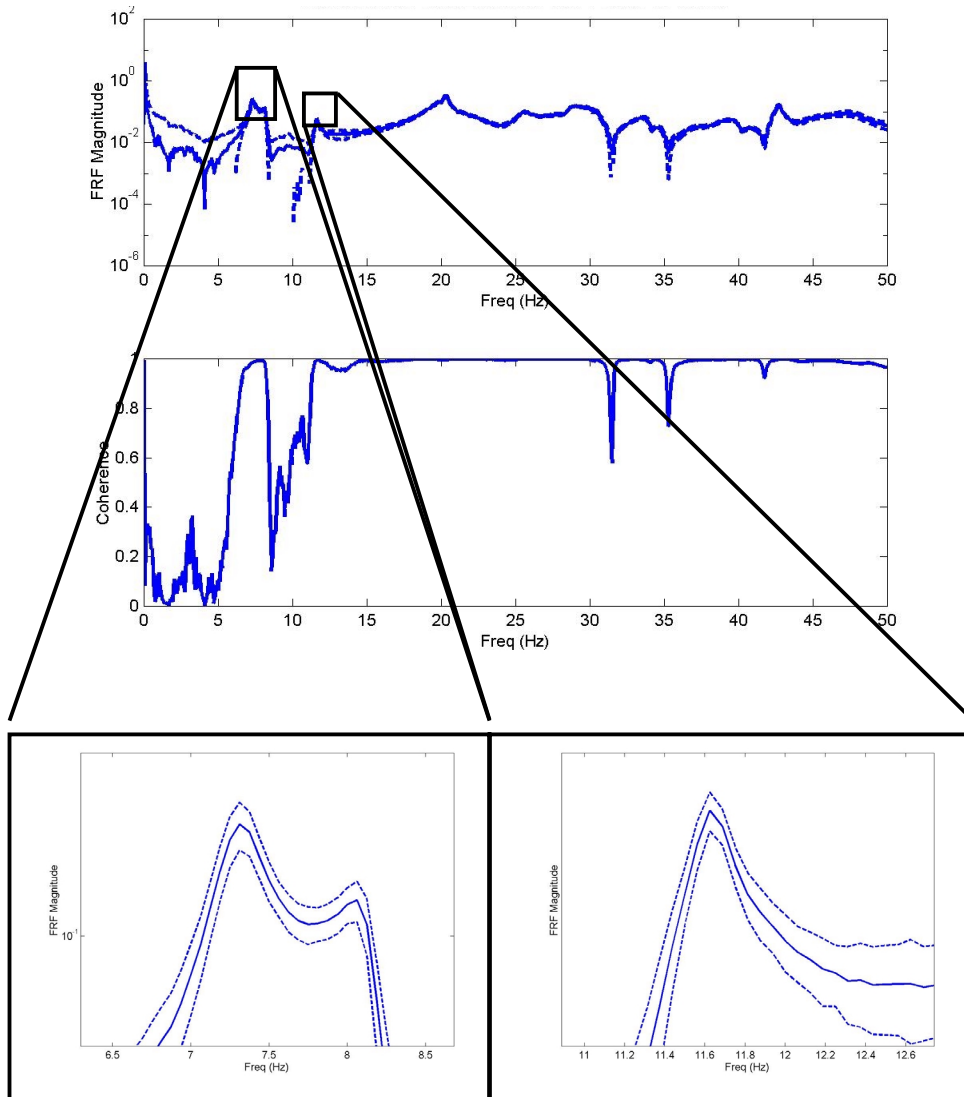


**Figure 12: Frequency Response Function Bounds (2 STD) from Alamosa Canyon Bridge Test  
(with Coherence)**

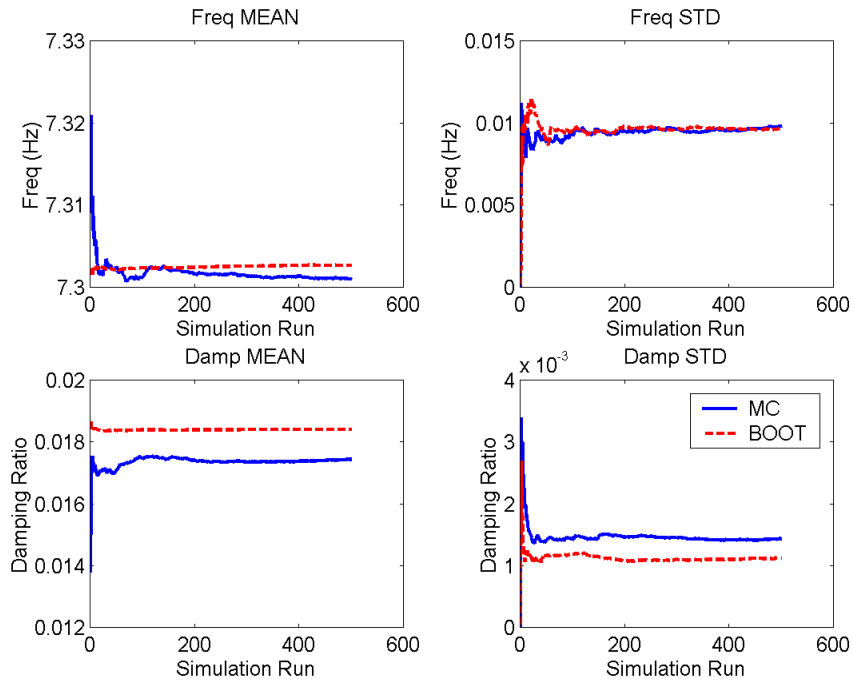


**Figure 13: Convergence of Modal Parameter Statistics for Alamosa Canyon Frequency Response Data**

**(Mode 1)**

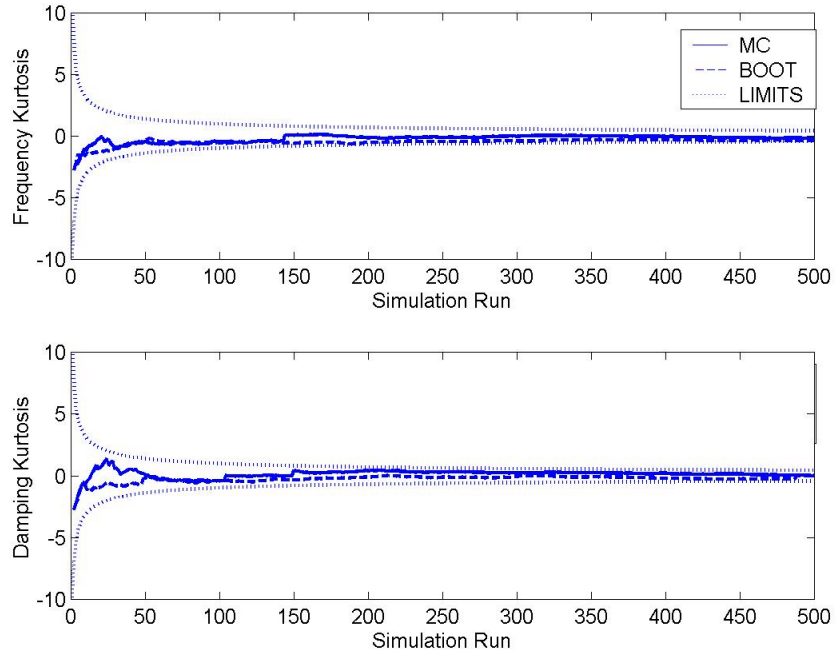


**Figure 14: Convergence of Modal Parameter Kurtosis for Alamosa Canyon Bridge Data**

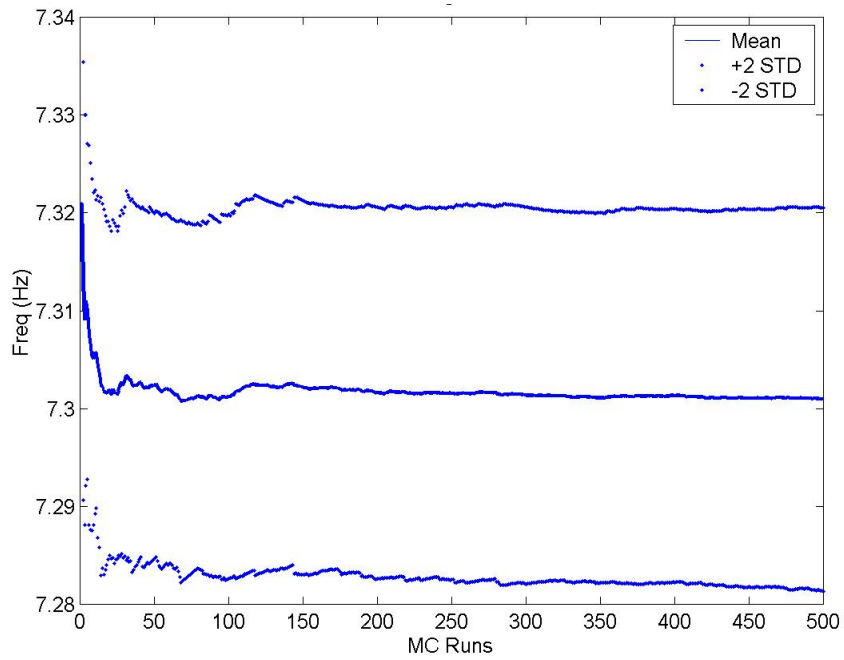


**Figure 15: Convergence of First Modal Frequency for Alamosa Canyon Bridge Data (Monte Carlo Method)**

## LIST OF TABLE AND FIGURE CAPTIONS

**Table 1: Statistics of Identified Parameters for Random Simulated FRFs**

**Table 2: Statistics of Identified Parameters for Alamosa Canyon Bridge FRFs**

**Figure 1: Flowchart of Bootstrap Procedure for Estimating Statistical Distributions**

**Figure 2: Flowchart of Monte Carlo Procedure for Propagating Statistical Distributions**

**Figure 3: Simulated Frequency Response Functions for Bootstrap Analysis**

**Figure 4: Simulated Frequency Response Function Bounds (2 STD) for Monte Carlo Analysis**

**Figure 5: Convergence of Modal Parameter Statistics for Simulated Frequency Response Data**

**Figure 6: Convergence of Modal Parameter Kurtosis for Simulated Frequency Response Data**

**Figure 7: Convergence of First Modal Frequency for Simulated Frequency Response Data**

**Figure 8: Elevation View and Cross Section of the Alamosa Canyon Bridge**

**Figure 9: Sensor Layout for Alamosa Canyon Bridge Tests**

**Figure 10: Variability of First Modal Frequency with Time and Temperature Differential**

**Figure 11: Individual FRF Samples from Alamosa Canyon Bridge Test**

**Figure 12: Frequency Response Function Bounds (2 STD) from Alamosa Canyon Bridge Test (with Coherence)**

**Figure 13: Convergence of Modal Parameter Statistics for Alamosa Canyon Frequency Response Data (Mode 1)**

**Figure 14: Convergence of Modal Parameter Kurtosis for Alamosa Canyon Bridge Data**

**Figure 15: Convergence of First Modal Frequency for Alamosa Canyon Bridge Data (Monte Carlo Method)**